Spatiotemporal Variations of Lake Surface Temperature across the Tibetan Plateau Using MODIS LST Product

Article *in* Remote Sensing · October 2016

DOI: 10.3390/rs8100854

CITATIONS
5

READS
103

7 authors, including:

Kaishan Song
Northeast Institute of Geography and Agroecology, Changchun, China.
10 PUBLICATIONS **72** CITATIONS
SEE PROFILE

Jia Du
Chinese Academy of Sciences
70 PUBLICATIONS **515** CITATIONS
SEE PROFILE

Ma Jianhang
Chinese Academy of Sciences
10 PUBLICATIONS **58** CITATIONS
SEE PROFILE

remote sensing

MDPI

Article

Spatiotemporal Variations of Lake Surface Temperature across the Tibetan Plateau Using MODIS LST Product

Kaishan Song *, Min Wang, Jia Du, Yue Yuan, Jianhang Ma, Ming Wang and Guangyi Mu

Northeast Institute of Geography and Agroecology, CAS, Changchun 130102, China; 15590684233@163.com (M.W.); jiaqidu@iga.ac.cn (J.D.); Yuanyue@126.com (Y.Y.); mmjjhh105@126.com (J.M.); w.m9047@163.com (M.W.); mugy390@nenu.edu.cn (G.M.)

* Correspondence: songks@iga.ac.cn; Tel.: +86-431-8554-2364

Academic Editors: Ruiliang Pu, Xiaofeng Li and Prasad S. Thenkabail

Received: 13 June 2016; Accepted: 12 October 2016; Published: 17 October 2016

Abstract: Satellite remote sensing provides a powerful tool for assessing lake water surface temperature (LWST) variations, particularly for large water bodies that reside in remote areas. In this study, the MODIS land surface temperature (LST) product level 3 (MOD11A2) was used to investigate the spatiotemporal variation of LWST for 56 large lakes across the Tibetan Plateau and examine the factors affecting the LWST variations during 2000–2015. The results show that the annual cycles of LWST across the Tibetan Plateau ranged from −19.5 °C in early February to 25.1 °C in late July. Obvious diurnal temperature differences (DTDs) were observed for various lakes, ranging from 1.3 to 8.9 °C in summer, and large and deep lakes show less DTDs variations. Overall, a LWST trend cannot be detected for the 56 lakes in the plateau over the past 15 years. However, 38 (68%) lakes show a temperature decrease trend with a mean rate of −0.06 °C/year, and 18 (32%) lakes show a warming rate of (0.04 °C/year) based on daytime MODIS measurements. With respect to nighttime measurements, 27 (48%) lakes demonstrate a temperature increase with a mean rate of 0.051 °C/year, and 29 (52%) lakes exhibit a temperature decrease trend with a mean rate of −0.062 °C/year. The rate of LWST change was statistically significant for 19 (21) lakes, including three (eight) warming and 17 (13) cooling lakes for daytime (nighttime) measurements, respectively. This investigation indicates that lake depth and area (volume), attitude, geographical location and water supply sources affect the spatiotemporal variations of LWST across the Tibetan Plateau.

Keywords: MODIS imagery; bulk temperature; Tibetan Plateau; water supply source

1. Introduction

Lake water surface temperature (LWST) has been regarded as a critical parameter in controlling functioning processes in aquatic ecosystems, e.g., physical, chemical and biological processes [1,2], and serious ecological consequences may be caused by lake warming [3,4]. As demonstrated by [5], some of the large lakes across the world show obviously increasing temperature as a result of climate change [6]. For example, the surface temperature of Lake Baikal, the deepest lake in the world increased by about 1.2 °C since 1946 [7]. Lake temperature reflects its morphology, watershed and hydrological conditions and eventually influences aquatic organisms [8,9]. Conventional approaches to measurement of lake water temperature use in situ data loggers to measure LWST. While such measured information is temporally continuous, its application for capturing temperature variations at large scale is constrained because of its limited spatial coverage [9]. Synoptic information is needed to map the sources of thermal heterogeneity at the watershed scale and examine the influence of the thermal variation across lake surface that may influence biophysical-chemical processes for a specific water body [10–12].

Lake water temperature is mainly influenced by the absorption of solar energy, which depends on an array of physical, chemical, and, to some extent, biotic properties of waters being concerned [1,13]. LWST changes seasonally due to the annual insulation and the variation of air temperature [1,9,14,15]. The amount of light absorbed by water increases exponentially with the distance of the light traveling through the water column, particularly those at wavelengths shorter than 750 nm [6,14]. High specific heat of water permits the dissipation of light energy and is accumulated as heat in the water column. However, heat retention is coupled with a number of factors that influence its distribution within lake systems, e.g., the wind speed, currents and other water movements, the morphology of watersheds, and gains and losses of water [13,14]. Thus, the pattern of thermal evolution and stratification fundamentally influences the physical and chemical cycles of lakes, which in turn govern lake production and decomposition processes [8].

Thermal remote sensing provides a synoptic context for evaluating the relationships between landscape and water thermal characteristics [4,16,17], and has been widely applied for mapping LWST and the circulation pattern of lakes [12,18]. For example, NOAA/AVHRR and Moderate Resolution Imaging Spectroradiometer (MODIS) on board Terra/Aqua has been widely used for monitoring lake surface temperature [19,20], while a bunch of investigations have used Landsat-TM/ETM+/OLI and ASTER for retrieving the thermal features of inland and coastal sea waters [4,18].

Known as the world "Third Pole" and the "Asian Water Tower", the Tibetan Plateau has experienced obvious climatic change in the past several decades [21,22]. Consequently, the cryosphere and hydrologic environment have substantially changed on the plateau [22–24]). However, few studies have been conducted to map LWST in alpine environments like the Tibetan Plateau where the elevated land surface temperature may raise LWST of this region [9,20]. In this study, the LWST pattern of 56 lakes in the Tibetan Plateau was examined to determine its association with landscape variations, hydrologic conditions and relief gradients. The objectives of this study are to: (1) examine the LWST variations of lakes across the Tibetan Plateau by using time series MODIS LST data; (2) compare the seasonal behavior of WST for water bodies with various morphological conditions; and (3) examine the potential impact factors that regulate the spatial and seasonal WST variations.

2. Materials and Methods

2.1. Study Area

The Tibetan Plateau is an extensive elevated plateau in China, covering an area about 2.5 million km^2. Endorsed with high elevation and tens of thousands of glaciers, the plateau is the headwaters of the drainage basins for most of the rivers in the surrounding regions. The impact of global warming on the Tibetan Plateau is of intense scientific interest [20,22]. Annual precipitation ranges from 100 to 1300 mm and falls mainly as rainfall, snow and hailstorms [23]. Proceeding to the north and northwest, the plateau becomes progressively higher, colder and drier, until reaching the remote Changthang region in the northwestern part of the plateau, where the average elevation exceeds 5000 m and winter temperatures can drop to −40 °C.

Thousands of closed lakes have developed on the Tibetan Plateau, and the total area is approximately half of the lake area in China [20], and most of which is sensitive to global warming [22,24]. Mainly fed with snow and glacier melting waters, some closed lakes are experiencing expansion in summer and autumn, which is more obvious when lakes are supplemented with glacier melting waters [22,24]. Lake surface temperature drops progressively from late autumn to winter, and begin to freeze in late November or December, and ice-off generally begins in April or May of the following year. Influenced by various geographical settings, elevation and climatic conditions, lake surface area and water volume show different responses to climate variability, while the response of LWST is yet not fully understood [25].

2.2. MODIS Imagery and Processing

Due to the limited number of valid pixels in the MODIS daily LST product [12], we use the MODIS LST 8-day composite product (level 3, MOD11A2), which integrates the average of daily LST observations in eight days with a nominal resolution of 1 km^2. The data temporal span is 16 years starting from 1 June 2000 to 31 December 2015. According to previous studies, the MODIS LST products over lake surfaces were evaluated with in situ measured temperature, and the absolute differences between MODIS derived and in situ measurements ranged from 0.8 to 1.9 K [26,27]. The MODIS Reprojection Tool (MRT, Land Processes DAAC, 2008) was used to extract 8-day composite LST data from 5 grid tiles and to cover the Tibetan Plateau. With limited direct field temperature measurements, the validation of MODIS LST products was conducted by following two approaches. The MODIS products with quasi-concurrent field survey were validated with direct temperature measurements over lakes collected in 2014 and 2015. In addition, the reliability of MODIS LST was also validated via comparing MODIS LST time series values with ground surface temperature (GST) at 0 cm measured over five weather stations distributed across the Tibetan Plateau (Figure 1), which is proven to be an effective method to assess LWST over Lake Siling Co [12].

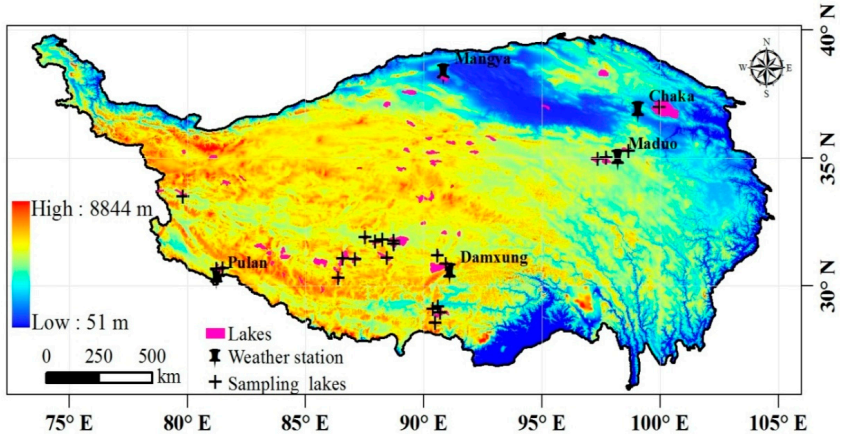

Figure 1. The distribution of lakes (>50 km^2) concerned and the stations for validation dataset collection across the Tibetan Plateau.

2.3. Methods for Lake Skin Temperature Characterization

After mosaicking by use of MRT, 8-day composite MODIS LST images were projected to Albers in GeoTIFF format with the nearest neighbor interpolation method. Four layers were extracted from LST product, i.e., daytime LST (overpass time is about 10.30 a.m. of local time), nighttime LST (overpass time is about 22.30 p.m. of local time) and corresponding quality control images (QC-daytime and QC-nighttime). Due to the strong contrast between land and water spectral features in near infrared (NIR) and green bands, a threshold was used to extract water body boundaries based on the NIR/Green ratio of Landsat TM images. The boundary shape file was generated for lakes with surface area greater than 50 km^2 (56 lakes) using Landsat TM images mainly acquired in 2008 and making reference to the MODIS reflectance product (MOD09Q1). To avoid errors resulting from the fluctuation of the land-water interface, a 1-km buffer zone offshore was generated to exclude LST pixels along shoreline zones [12].

Although the 8-day composite product was utilized in the study, cloud contamination still exists and an appropriate procedure should be taken to remove problematic pixels [12,26]. The method proposed by [12] was adopted to remove unreliable LST pixels over lakes using QC information and median filtering of time series LST data stacks. With reference to the LST data quality flag files stored in QC file, all pixels that have averaged LST errors less than 1K (i.e., QC = 0, 1, 5, 17, 21), pixels with other QC values were removed. In the second step, a data cube was generated through stacking 46 layers

of LST according to the day-of-year sequence, and then filtered by application of median filtering algorithms to eliminate problematic pixels in the LST images (see supplementary Figure S1). For most of the cases considered here, the 8-day composite contains valid pixels greater than 70%, and only 37 out of 1472 images (2.5%) in the past 16 years contained valid pixels less than 70% (Figure S2). The presence of monthly effective images followed a similar temporal pattern when all the years considered (Figure S3). More effective images were identified from April to June, and September to mid-December. Furthermore, more effective images were also found from the nighttime MODIS LST product (Figure S3), which is consistent with the findings from other investigations [12,20,26].

2.4. Definition and Calculation of LWST

The mean LWST is derived by averaging all pixels of daytime or nighttime LST images composited in a specific period for a given lake. With respect to monthly (e.g., freeze-up and break-up month) and annual LWST for the daytime or nighttime SWT, the mean was derived by aggregating the 8-day LWST composite for the corresponding time series [12]. Diurnal temperature differences (DTDs) of LWST were derived with daytime temperatures subtracted by nighttime ones. For each year, the ice break-up month starting point was determined through referencing to day-night averaged LWST of 56 lakes above 0 °C, and four 8-day LWST consecutive MODIS measurements were accounted since then. The warm month across the Tibetan Plateau starts from the end of July to mid of August with referencing to the highest day-night averaged LWST of 56 lakes in each year. The freeze-up month ending point was determined through referencing to day-night averaged LWST of 56 lakes about 0 °C for each year, four 8-day LWST consecutive measurements before that point were accounted as the freeze-up month.

The intra-annual variation of LWST was analyzed by averaging daytime and nighttime SWT time series of ice-free seasons in the past 16 years. In each year, the annual average LST maps were the average of ice-free season 8-day maps calculating via pixel-by-pixel. In addition, ice break-up, freeze-up date, and ice-free duration having direct connection with LWST, were also calculated through counting the accumulative days of the mean temperature ((daytime + nighttime)/2) above, below 0 °C for each of the 56 lakes concerned, where the median of the Julian Day for each 8-day composite was considered for accumulative days counting. Further, to track the temporal trend of LSWT for each of the 56 lakes, the rate of temperature annual change from MODIS LST data was regressed against the data acquisition year using the following regression model [20]:

$$y = a + bx + e \quad (1)$$

where y represents the MODIS LST, x denotes the time series of years, e represents the residuals, a is the intercept, and b is the rate of temperature change; a and b are determined through least squares fitting.

3. Results

3.1. Validation of LST MODIS Product

3.1.1. Validation by in Situ Measured Data

In situ measurements were carried out in 2014 and 2015 in some of the lakes (Figure 1) using YSI portable probes (YSI Inc., Yellow Spring, OH, USA) placed in open water at a depth of 0.3 m, and the sampling time ranged from 9:00 a.m. to 4:00 p.m. local time. Although in situ measurement of water surface temperatures at different stations were not coincident with the MODIS overpass time, the data were still used here due to the scarcity of the validation dataset. The MODIS images were selected if the field survey day fell within one of the eight-day composite. Altogether, 26 stations match up with the MODIS LST products during these surveys, and the average of each 3 × 3 pixel window was extracted and compared with in situ measured temperatures. The scatter plot of LWST versus in situ measured lake water surface temperature shows a cool bias (LWST-in situ) of 1.74 °C

and a root mean squared error (RMSE) of 2.8 °C (Figure 2a). Apart from known potential error sources, including instrumental noise and drift, sunlint, cloud contamination, and surface emissivity effects [26,28], a major source might be due to mismatch up between the timing of the in situ measured data and MODIS over-passing, which was further interfered by the eight-day composite. As argued by [25] that the differences in the observation time between satellites and in situ measurements may induce some deviations, the MODIS-derived LWST still showed its applicability in characterizing the thermodynamic features of the lakes across remote areas with harsh environmental settings. Further, considering the validation work over Lake Titicaca by [26], good performance of MODIS LST is expected over the plateau due less aerosol interfering with the path radiation. Thus, the eight-day MODIS LST composite is applicable for investigating the lake water temperature over the plateau.

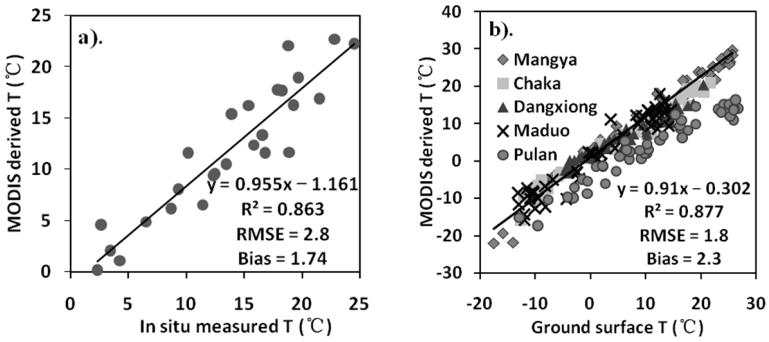

Figure 2. MODIS land surface temperature (LST) product validation with both in situ measured data (**a**); and meteorological data (**b**) were collected in five different stations while in situ data were measured in 15 lakes across the Tibetan Plateau in 2014 and 2015.

3.1.2. Validation by Meteorological Data

The GSTs from five meteorological stations of different elevations were used to validate the eight-day composited LST product (see Figure 1 for locations). The averaged pixel values of a 3 × 3 window centered at each meteorological station were extracted and were regressed against the corresponding GST values. As shown in Figure 2b, a relative high overall coefficient of determination (R^2 = 0.88) and low RMSE (1.8) were achieved for the pooled GST dataset, with a bias of 2.3 °C. According to the regressions between MODIS derived LST and GST, the slopes and R^2 varied for different stations. The Mangya station, located in west of Lake Gas Hure (see Figure S4) and the lowest elevation station (3500 m) selected for validating the MODIS LST product, showed good consistency between MODIS derived LST and GST (y = 1.091x + 0.87, R^2 = 0.977, Bias = 1.14). Likewise, the Chaka station also exhibited good performance (y = 0.925x + 0.968, R^2 = 0.979, Bias = 1.38), but the slope is not close to unity. According to the result obtained from the Maduo Station, the MODIS LST still showed stable performance (y = 1.053x − 0.184, R^2 = 0.903, Bias = 2.57). However, both the Dangxiong (y = 0.772x + 1.593, R^2 = 0.937, Bias = 3.4) and Pulan (y = 0.769x − 4.729, R^2 = 0.917, Bias = 4.7) stations exhibited large biases by showing lower slope values far from unity (see Figure 1 and Figure S4 for location). The large discrepancy between GST and MODIS LST for stations Dangxiong and Pulan may result from the heterogeneity of the landscape. Further, the instrument deployment depth may also cause the discrepancy between GST and MODIS-derived LST. As argued by [12], it is reasonable to expect that the quality of MODIS LST over water bodies is better than that over land surfaces since lake surfaces are rather homogenous, thus both spatial and temporal variations are more stable than that of land due to the larger heat capacity and less varied emissivity [25]. Thereby, the stable performance of the MODIS LST product justifies this investigation to the thermal characteristics of lakes across the Tibetan Plateau, where very limited field surveys were conducted for monitoring the lake water temperature features [21]. Further, the relative temperature trend rather than absolute temperature is more concerned of lakes across the plateau in this study.

3.2. Spatial Pattern of Lake Surface Temperature

3.2.1. LWST Pattern of Lakes across the Tibetan Plateau

The spatial temperature pattern of the month after ice break-up (Julian Day 114 to 144) is demonstrated in Figure 3. A large spatial variation was observed for LWST, ranging from −2.0 to 14.0 °C (Figure 3a), the coldest one was recorded in Nam Co, and the warmest one was measured with in Lake Yamdrok (see Figure S4 for locations). In general, warmer lakes were situated in the southern part of the plateau, while relative low temperature lakes were located in the Hoh Xil region. It can be noted that shallow lakes exhibited relative high temperature, i.e., Lake Dabsun, and Lake CuoE, which are close to Lake Siling Co (Figure S4). With respect to the nighttime temperature pattern, it can be observed in Figure 3b that low LWST was still exhibited with lakes in the Hoh Xil region, while warm temperature was recorded in Lake Dabsun and Gas Hure. Lake Qinghai and Ayakekumu in the north and those lakes locating in the southern part of the plateau showed relatively high temperature during the nighttime (see Figure S4 for locations). As expected (Figure 3c), large spatial variations of diurnal temperature differences (DTDs) were demonstrated for lakes across the plateau. Small DTDs were observed for large and deep lakes, e.g., Lake Qinghai, Nam Co, Siling Co, and Ayakekumu, large DTDs were generally found for small ones located in the south and west of the plateau, and those intermediate DTDs were found for lakes mainly located in the Hoh Xil region (see Figure S4 for locations).

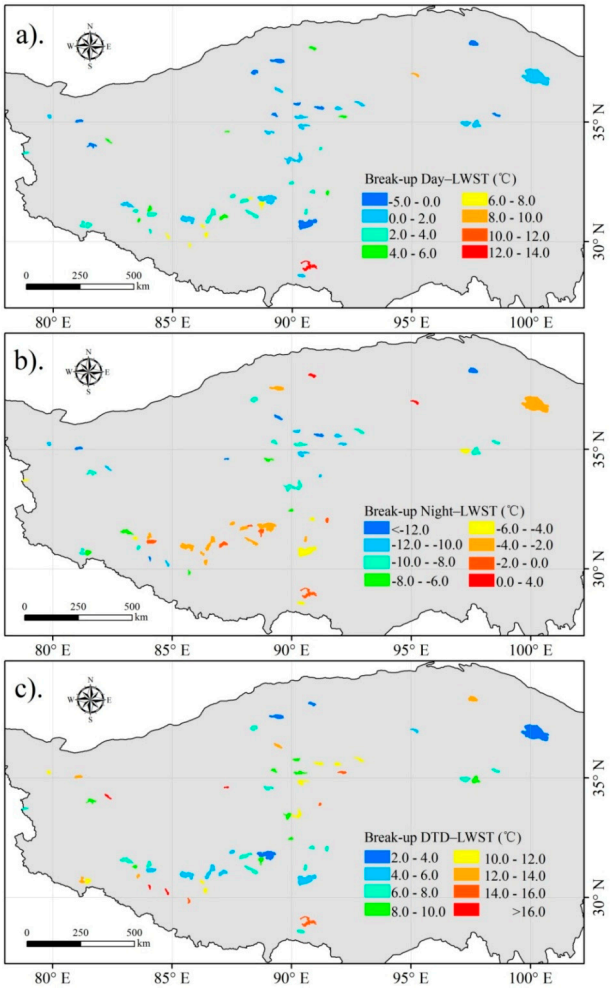

Figure 3. Spatial pattern of the monthly averaged water surface temperature after ice break-up month: (**a**) daytime lake water surface temperature (LWST) variation; (**b**) nighttime LWST variation; and (**c**) lake water surface diurnal temperature difference (DTD).

The spatial pattern of LWST for lakes in the warm month (Julian Day 200–232, a good indicator for the highest LWST reached in the region) was demonstrated in Figure 4, with temperature ranging from 10 to 28.7 °C for the daytime, and 3.0 to 19.0 °C for nighttime. As shown in Figure 4a, the warmest temperature was found in Lake Dabsun and CuoE in the low elevation region in the north part, and some lakes in the southern part of the plateau. Lakes in the Hoh Xil region, and Nam Co, PumuYumco exhibited low temperature (10–12 °C). In general, the spatial pattern of LWST derived from the nighttime MODIS product resembled that in daytime; however, Lake Yamdrok showed much lower nighttime temperature (Figure 4b). Combination of both daytime and nighttime LWST patterns indicates that large and deep lakes with huge water storage showed less variability for DTDs, i.e., Lake Qinghai, Nam Co, Siling Co and Ayakekumu. As demonstrated in Figure 4c, Lake Yamdrok Co, and Langa Co and other two relatively small lakes showed much larger DTD variability, ranging from 6 to 9 °C.

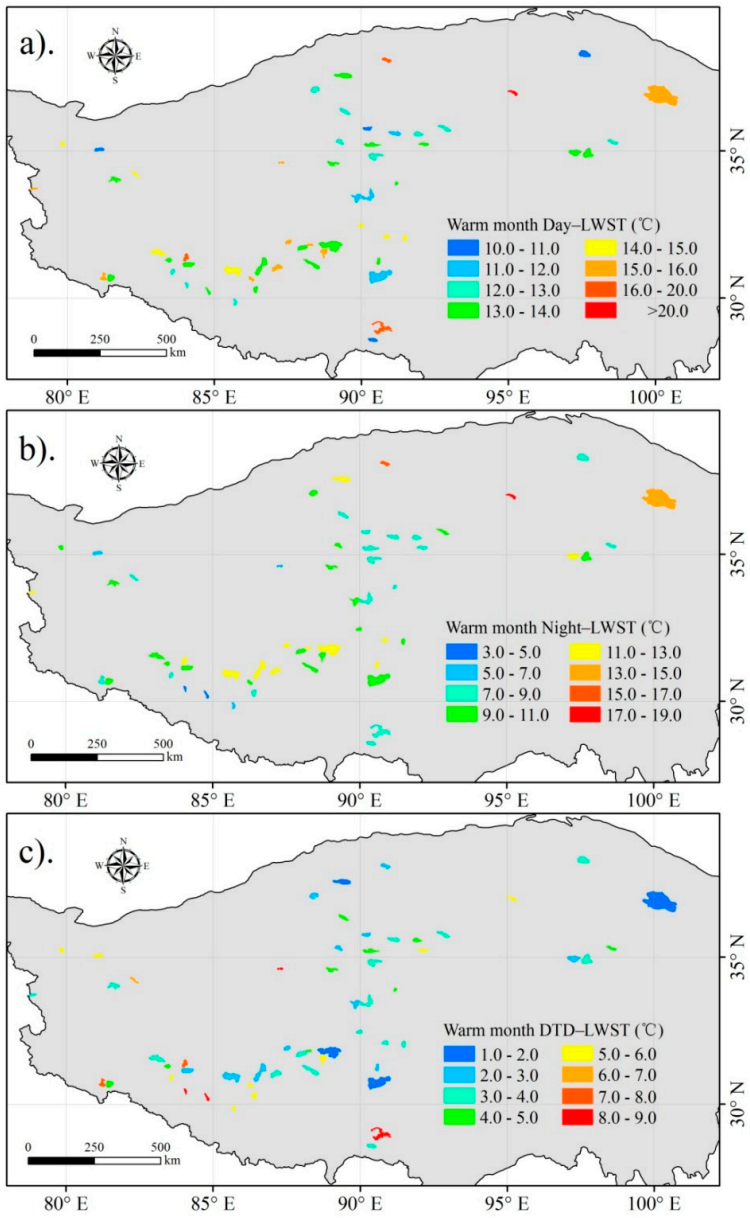

Figure 4. The warm month spatial pattern of water surface temperature for lakes across the Tibetan Plateau: (**a**) daytime LWST variation; (**b**) nighttime LWST variation; and (**c**) lake water surface diurnal temperature difference (DTD).

The spatial pattern of monthly LWST for lakes before completely frozen (304–336) in the Tibetan Plateau was presented in Figure 5. A very obvious spatial pattern of LWST was evident in the daytime MODIS LST product. It can be seen that Lake Qinghai had a large storage at low elevation, and lakes in the southern part of the plateau exhibited warmer temperature, ranging from 1 to 6.8 °C before the presence of ice. Lakes situated across the Hoh Xil region and the western part of the plateau had low temperatures, ranging from −9 to −1 °C. Almost a similar pattern of LWST was exhibited for lakes across the plateau during the nighttime. A comparable DTD pattern was revealed as that from ice break-up and the warm periods, i.e., smaller DTDs were found with large and deep lakes, e.g., Lake Qinghai, Nam Co, Siling Co, MapamYumco, and Ayakekumu, while large DTDs were recorded with Lake Yamdrok, and those situated in the Hoh Xil region (see Figure S4 for locations).

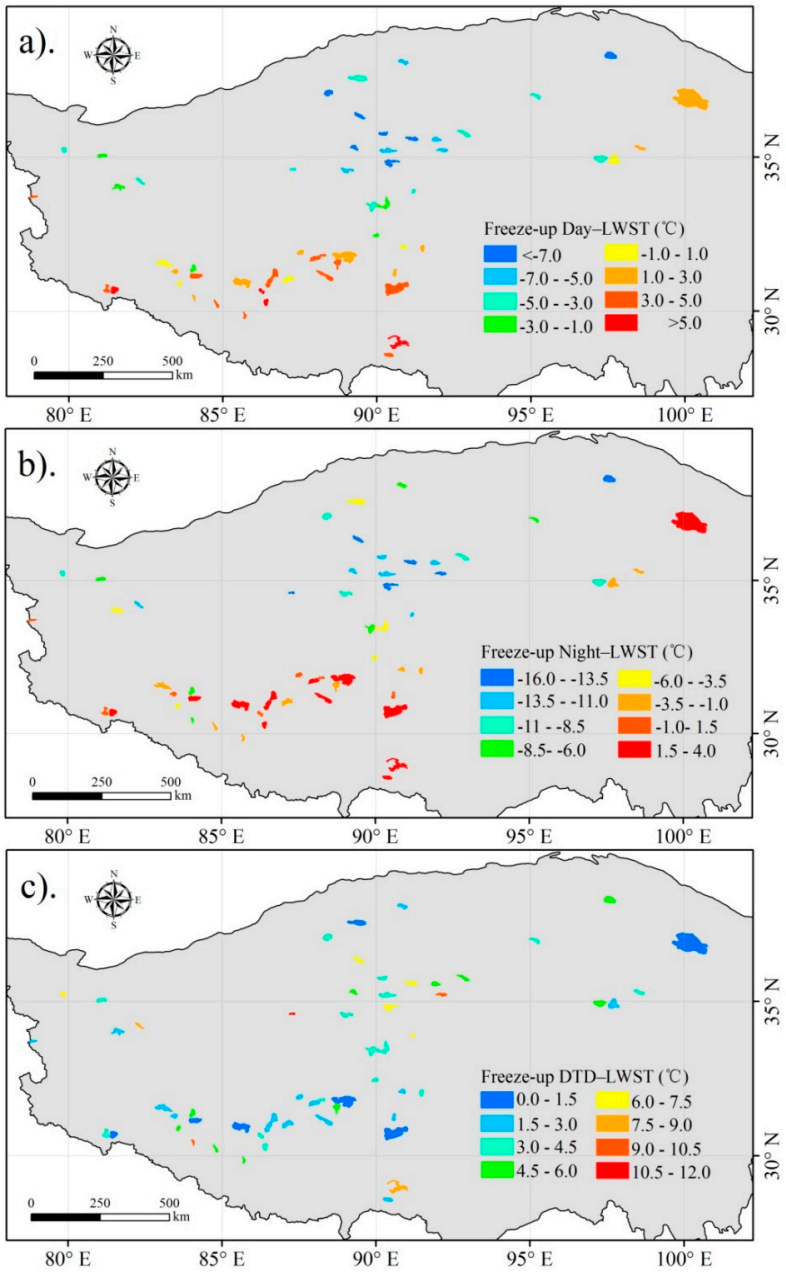

Figure 5. The spatial pattern of the monthly averaged water surface temperature before freeze-up period in Tibetan Plateau: (**a**) LWST daytime variation; (**b**) LWST nighttime variation; and (**c**) lake water surface diurnal temperature difference (DTD).

3.2.2. Water Surface Temperature Variation for Typical Lakes

As shown in Figure 6, apparent internal variations for LWST were demonstrated with respect to different lake sizes, attitudes and water supply sources. Located at the lower elevation (Table 1), Lake Qinghai demonstrated higher temperature with obvious internal temperature variation (Figure 6a). The temperature is high in the mid-north and northeast regions for the daytime and in the northeast region for the nighttime. The mean temperature generally resembles the temperature in nighttime. Likewise, the temperature in Siling Co displays high values in the south and north shoreline border regions (Figure 6b), but less variability in the open water region. Located in the high elevation Hoh Xil region, the temperature of Lake Hoh Xil was low and had larger spatial variability (Figure 6d). While Lake MapamYumco and Langa Co are spatially close, higher internal spatial variability was presented in Langa Co due to its shallow water depth and much complex shoreline (Figure 6e). The temperature pattern in Lake Gyaring resembles that in Lake Ngoring, but statistical analysis suggested a little bit higher temperature presented in Lake Gyaring due to shallow water depth (Figure 6f and Table 1). Because of shallow water depth and high salinity, Lake Dabsun showed the highest temperature across the plateau (Figure 6g). Located in the southern part of the plateau, Lake Yamdrok also exhibited high water temperature with strong internal variation (Figure 6h).

Table 1. Limnological characteristics of typical lakes across the Tibetan Plateau for water surface temperature comparison.

Name	WL (m)	A (km^2)	AD (m)	Supply	V (10^8 m^3)	Salinity (PSU)
LakeQinghai	3194	4340	21.3	R + P	738.6	14.7
Nam Co	4718	1961	57.6	G + R + P	863.7	0.9
Siling Co	4530	2175	33.5	G + R + P	-	18.3
CuoE	4561	269	7.8	R + P	-	261
Ayakekumu	3876	927	12.3	G + R	-	145.9
Yamdrok	4441	638	43.5	R + P	151.0	1.7
Pumu Yumco	5010	290	47	G + R + P	133.5	0.37
Dangre Yumco	4528	835.3	93	G + R + P	576.5	9.7
Taruo Co	4566	515.6	-	G + P	-	110.7
Langa Co	4572	268	31.4	G + R + P	57.1	0.7
MapamYumco	4586	412	47.3	G + R + P	146.2	0.2
Gyaring Hu	4292	526	8.9	R + P	46.7	0.5
Ngoring Hu	4269	610	17.6	R + P	107.6	0.3
Hoh Xil	4878	300	30.7	G + R	58.6	13.4
UlanUla	4854	544	6.9	G + P	-	10.9
Akesaiqin	4848	185	16	R + P	-	54.8
Dabsun	2675	257	1.02	R + P	2.6	320.2

Note: WL, water level; A, area; AD, average depth; V, volume; R, river; G, glacier melting water; P, precipitation over lake surface; - not applicable.

As demonstrated in the right column of Figure 6, the DTDs of the shoreline regions for different lakes had much larger variability, particularly for these with elongated shapes (e.g., Lake Hoh Xil and Lake Langa). It also revealed that lakes having large area and in deep basins showed less internal variability, e.g., Lake Qinghai and Siling Co. As an extreme case, Lake Dabsun also demonstrated a large DTD variation from shoreline toward the central part of the lake surface. Similarly, Lake Yamdrok, a narrow lake in a complex lake basin, demonstrated larger DTDs.

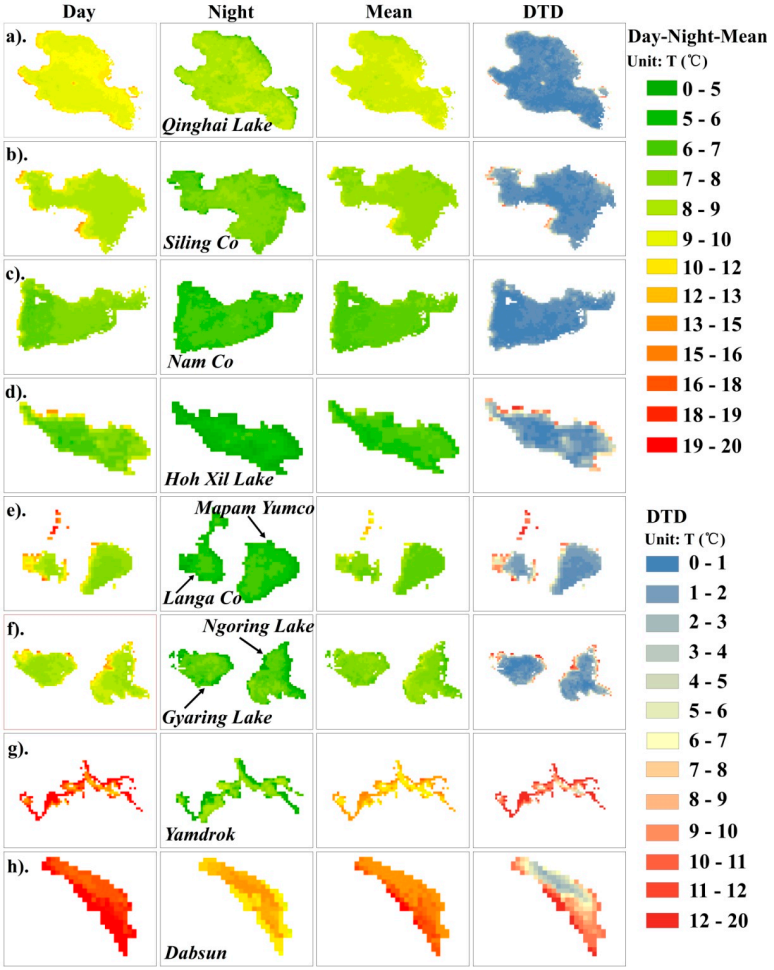

Figure 6. The spatial LWST patterns for eight typical lakes during ice-free period, column one to three are averaged daytime, nighttime, and mean of day-nighttime temperature, while column four is the averaged diurnal temperature difference (DTD): (**a**) Qinghai Lake; (**b**) Siling Co; (**c**) Nam Co; (**d**) Hoh Xil Lake; (**e**) Mapam Yumco and Langa Co; (**f**) Ngoring Lake and Gyaring Lake; (**g**) Yamdrok; (**h**) Dabsun Lake.

3.3. Temporal Variation of Lake Surface Temperature

3.3.1. Intra-Annual Variation of LWST

As demonstrated in Figure 7, the overall temperature increased from the beginning of February, and the daytime temperature was about 0 °C in the mid of March (approximately Julian Day 70), while the nighttime temperature reached 0 °C in the beginning of May (approximately Julian Day 128). Overall, the warmest temperature of LWST reached in the early stage of August. The timing of lake ice cover break-up and freeze-up is an important phenological proxy for biological and chemical processes [8]. The timing of the maximum temperature is the most active period for lake surface evaporation, and also probably the most productive period of a lake for which the productivity is limited by temperature. The average overall lake temperature drops to 0 °C at the end of November or beginning of December (approximately Julian Day 336), indicating the formation of ice. By averaging both daytime and nighttime MODIS product, the mean LWST of lakes ranged from −10.3 to 15.7 °C. As shown in Figure 7, the maximum DTD (11.3 °C) was recorded during the ice break-up period, gradually decreased till ice freeze-up occurs (5.1 °C), and then an increase trend followed. Statistics revealed larger DTDs in the ice-covered season than ice-free season (8.7 vs. 6.2 °C). [12] argued that

LWST is probably prone to large DTD due to change in heat flux between day and night since ice has much less specific heat capacity than water [27].

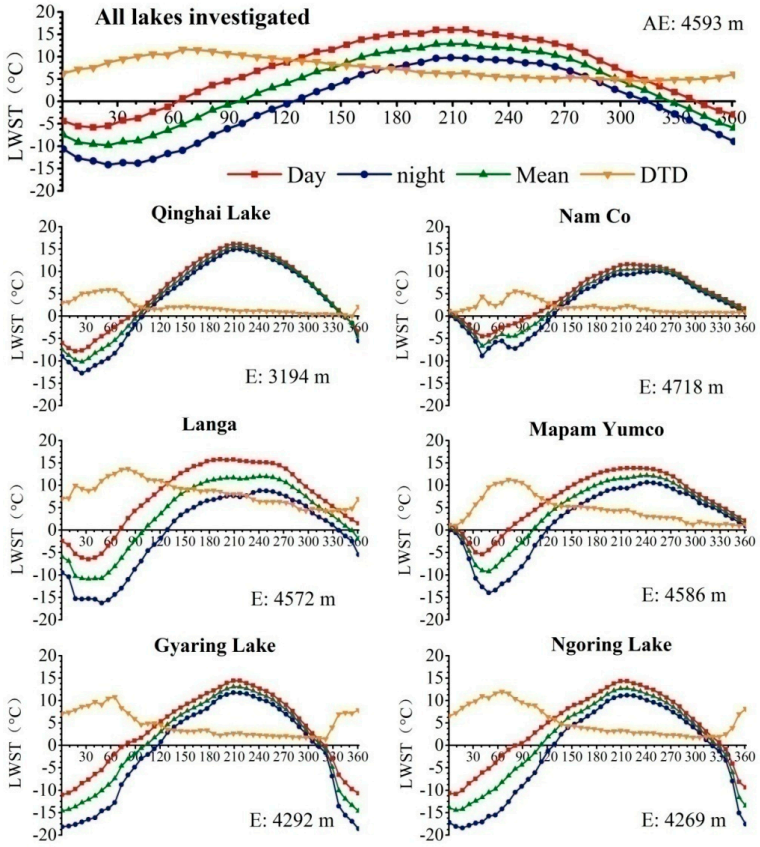

Figure 7. Fifteen-year averaged water surface temperature for daytime, nighttime and the mean value of day-nighttime temperature, and the diurnal temperature differences (DTD), the first row is derived from 56 lakes across the plateau, and the second to the fourth rows are results from typical lakes. E denotes the average elevation of 56 lakes above sea level in meter (m).

Over different lakes, the intra-annual variation of DTD followed a similar pattern, while the maximum DTD and the specific dates reaching the maximum DTD varied across different lakes (Figure 9). Lakes with large volume (large area or deep depth, or both) generally had a smaller DTD, e.g., Lake Qinghai and Nam Co (Table 1) both exhibited lower DTDs, with the maximum DTDs taking place before the ice break-up period. Lake Langa Co and MapamYumco are very close, but the former has much less volume (Table 1) and a much larger DTD and a longer ice-water duration period was recorded with Lake Langa Co. In terms of volume, Lake Gyaring is about half of Lake Ngoring, however, the two lakes had a similar trend for both daytime and nighttime DTDs. Through close examination of the maximum temperature, it can be found that Lake Gyaring is a little bit higher than Lake Ngoring. It also should be highlighted that the timing of the maximum DTDs for these specific lakes all occurred before the ice break-up period, ranging from Julian Day 72 to 88. The timing of the overall DTD was around Julian Day 72, but it is in the period when ice and water co-exists.

3.3.2. Variations of Ice Break-Up, Freeze-Up and Ice Free Duration

Ice break-up, freeze-up and ice-free duration have strong connection with LWST. The average daytime and nighttime temperatures were derived from each eight-day composite for 56 lakes concerned, and then break-up, freeze-up and ice-free duration were calculated. As shown in Figure 8a, the ice break-up dates varied significantly from lake to lake, ranging from Julian Day of 0 to 160

(standard deviation (SD) = 30.1 days). The two extreme cases are Lake Yamdrok and Xuru Co, which are ice-free during the study period according to the MODIS LST product. As an oppositecase, the lakes located in the Hoh Xil region in the northwestern part of the plateau exhibited late ice break-up dates, e.g., Lake Hoh Xil (160), and Lake Jingyu (152). Comparatively, shallow lakes with high salinity generally had earlier ice break-up date, e.g., Lake Dabsun (64) and Lake CuoE (64) (see Figure S4 for locations).

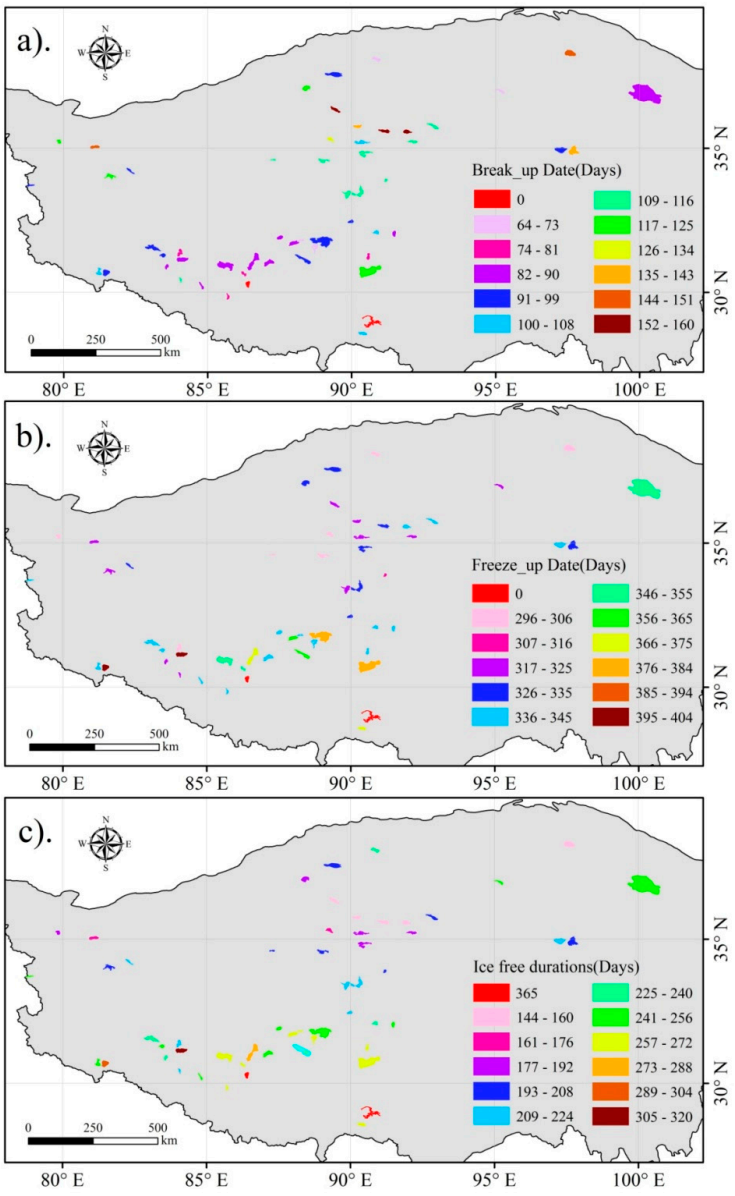

Figure 8. The timing variations of (**a**) ice break-up date; (**b**) freeze-up date and (**c**) ice-free durations for lakes across the Tibetan Plateau.

Comparatively, the freeze-up dates of different lakes showed less variation (SD = 23.0 days), ranging from Julian Day 304 to 32 of the following year, with the exception of Lake Yamdrok and Xuru Co (Figure 8b). Lake Hara, Akesaiqin, and Gas Hure in the northern part of the plateau exhibited earlier ice formation as air temperature went down at the end of fall and the beginning of winter. However, some lakes in the southern part of the plateau reveal much later ice formation dates, e.g., PumuYumco, Nam Co, and MapamYumco even showed freeze-up dates in January or early February in the following year (see Figure S4 for locations).

As shown in Figure 8c, a significant variation (S.D = 47.9 days) was demonstrated in the lake ice-free duration, ranging from 144 to 365 days. The lakes situated in the Hoh Xil region in the northwest with high elevation (exceeding 4500 m) exhibited shorter ice-free durations, e.g., Lakes Hoh Xil (144) and Jingyu (144) presented the shortest duration time for all the lakes investigated. As mentioned above, Lake Yamdrok and Xuru Co were the two extreme cases without ice formation according to MODIS derived LST measurements. Lakes with large volume generally exhibited a longer ice-free duration, e.g., Lake Qinghai, Nam Co. Likewise lakes situated in the southern part of the plateau, e.g., MapamYumco and DangreYumco, or lakes with high salinity also demonstrated longer ice-free time, e.g., CuoE and Taruo Co (see Figure S4 for locations and Table 1).

3.3.3. Inter-Annual Variation of WST for Lakes across the Tibetan Plateau

The inter-annual variations of the averaged LWST of lakes from 2001 to 2015 are demonstrated in Figure 9a. It can be seen that the annual daytime, nighttime co-varied during the past 15 years, with the highest being recorded in 2006 and the lowest in 2012. Although a slightly decrease trend can be observed during the study period, the trend of daytime and nighttime were insignificant. The corresponding parameters for the ice break-up period during the past 15 years are demonstrated in Figure 9b. An obvious decreasing trend was observed ($y = -0.110x + 3.827$, $R^2 = 0.304$, $p < 0.05$), while obvious trends could not be observed for nighttime and the mean value. However, an increasing trend was presented for both nighttime and the mean during 2001 to 2010, and an opposite trend followed from 2011 to 2015. As shown in Figure 9c, slight and coincident fluctuations were observed for daytime and nighttime of the warm months during the past 15 years, but no trends could be traced. Compared to the averaged daytime and nighttime temperatures of ice break-up and the warm month (Figure 9d), a significant increasing trend was observed during the freeze-up period during the past 15 years ($y = 0.047x - 0.906$, $R^2 = 0.125$, $p < 0.1$).

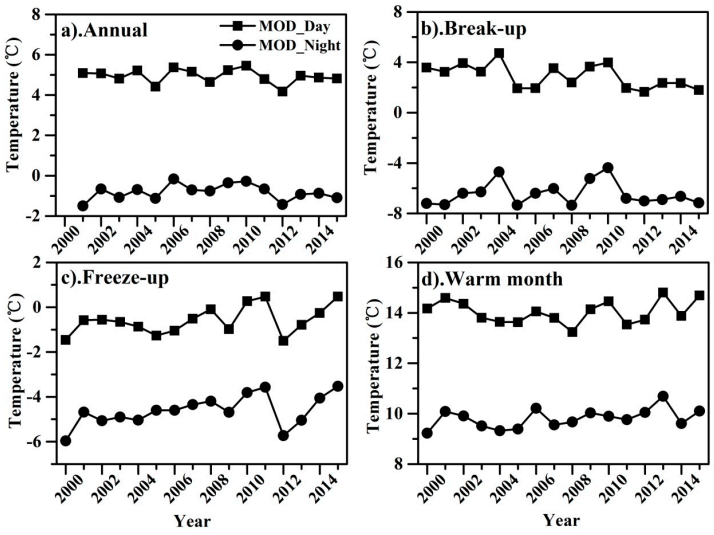

Figure 9. Inter-annual changes of lake-averaged annual daytime and nighttime water surface temperature (WST) of lakes from 2000 to 2015: (**a**) annual average; (**b**) break-up month; (**c**) freeze-up month; and (**d**) warm month.

The inter-annual variations of 56 lakes across the Tibetan Plateau from 2001 to 2015 are shown in Table 2. As can be seen, the daytime and nighttime trends for each lake exhibited various patterns, only 23 lakes showed consistent temperature trends in both daytime and nighttime during the past 15 years, and the rest exhibited an opposite trends from daytime and nighttime LST measurements. According to the daytime MODIS LST measurements, only 18 (32%) lakes showed increase in temperature with a mean rate of 0.04 °C/year, while the rest 38 (68%) lakes decreased in temperature

with a mean rate of −0.06 °C/year. Regression analysis indicated that the daytime LWST trend of 19 lakes is significant, including three warming and 16 cooling lakes (Table 2). With respect to nighttime MODIS LST measurements, 27 (48%) lakes increased in temperature with a mean rate of 0.051 °C/year, and 29 (52%) lakes decreased in temperature with a mean rate of −0.062 °C/year. The LWST change rate for 19 lakes was statistically significant, including seven warming and 12 cooling lakes for nighttime MODIS LST measurements. The number of lakes with warming rates is a little bit different from the findings by [20]. Altogether, 34 lakes were examined by both investigations; thus, further comparison was conducted on these lakes (Table S1). As seen in Table S1, 10 lakes increased consistently in temperature, while eight lakes consistently decreased in temperature. Sixteen lakes showed different temperature change rates, however, eight out of these lakes showed a consistent trend when the regression year was limited to 2001–2012 (Table S1 and reference [20]). Considering the low R-squares values in the regression models (Table S1), the remaining eight lakes with inconsistent trend can be ignored. Thus, the result from this investigation is consistent with the findings by [20].

Table 2. Lake water surface temperature change rates derived from MODIS LST regressing against year between 2001 and 2015 for both daytime and nighttime series data, these rates of temperature change in grey color are showing a cooling trend, while the rest showing warming trend.

Lake Name	Rate of Daytime WST (°C/year)	R^2	Rate of Nighttime WST (°C/year)	R^2
Tsonag Lake	0.043	0.12	0.044	0.07
Hara Lake	0.021	0.04	0.081	0.13
Qinghai Lake	0.024	0.04	0.044	0.10
Lumaqangdon Co	0.033	0.04	0.048	0.08
ZigeTangco	0.013	0.02	0.074 *	0.29
Gyaring Lake	0.004	0.00	0.072	0.10
Hoh Xil Lake	−0.143 **	0.37	−0.091 **	0.37
LexieWudan	−0.073 *	0.27	−0.088 *	0.28
ZhariNam Co	−0.041 *	0.23	−0.084 *	0.23
Ngangzi Co	−0.04 4*	0.20	−0.012	0.00
Dore Sowdong Co	−0.062 *	0.19	−0.044	0.05
Ringinyubu Co	−0.040 *	0.18	−0.051	0.14
DogaicoringQangco	−0.042	0.15	−0.013	0.01
Langa Co	−0.093	0.13	−0.143 **	0.30
Senli Co	−0.122	0.11	−0.073	0.14
Palung Co	−0.052	0.11	−0.087 *	0.20
PangongTso	−0.032	0.08	−0.033	0.08
MapamYumco	−0.061	0.07	−0.138 *	0.19
AngLaren Lake	−0.014	0.02	−0.024	0.07
GyesarTso	−0.013	0.01	−0.072 *	0.26
Gozha Co	−0.013	0.01	−0.022	0.01
Nam Co	−0.002	0.00	−0.054	0.08
Taro Co	−0.0003	0.00	−0.053 *	0.19
Yamdrok	0.143 **	0.55	−0.053 *	0.21
HuitenNur	0.171 **	0.45	−0.173 **	0.44
Xuru Co	0.054 *	0.28	−0.053 *	0.24
CuoE	0.041	0.10	−0.025	0.06
Mucuobingni	0.034	0.07	−0.083 *	0.22
Jargo Lake	0.034	0.06	−0.018	0.02
Urru Co	0.027	0.05	−0.044	0.13
Geren Co	0.011	0.02	−0.048	0.14
PumuYumco	0.013	0.02	−0.053	0.05
Zabuye Lake	0.023	0.02	−0.001	0.00
Dajia Lake	0.002	0.00	−0.124 *	0.24
DangreYumco	0.0023	0.00	−0.034	0.13
Akesaiqin	−0.142 **	0.63	0.032	0.12
Jingyu Lake	−0.132 **	0.46	0.024	0.02
Dogze Co	−0.071 **	0.42	0.044	0.20
Dabsun	−0.251 **	0.37	0.173 **	0.45
UlanUla	−0.088 **	0.36	0.064 *	0.18

Table 2. *Cont.*

Lake Name	Rate of Daytime WST (°C/year)	R^2	Rate of Nighttime WST (°C/year)	R^2
Gas Hure	−0.058 **	0.34	0.003	0.00
CoNyi	−0.134 *	0.29	0.138 **	0.46
MemarTso	−0.081 *	0.29	0.132 **	0.44
Hoh Sai Lake	−0.074 *	0.28	0.062 *	0.29
XijinUlan	−0.081 *	0.25	0.013	0.01
Quemo Co	−0.082 *	0.21	0.044	0.14
MirikGyangdramTso	−0.044	0.09	0.024	0.03
AqqikKol	−0.035	0.07	0.053	0.16
DonggiConag	−0.044	0.06	0.014	0.09
Siling Co	−0.013	0.04	0.034	0.09
Dogai Coring	−0.024	0.03	0.023	0.02
Ngoring Lake	−0.024	0.02	0.083	0.15
Dorge Co	−0.023	0.02	0.004	0.00
Ayakekumu	−0.009	0.01	0.011	0.01
Serlung	−0.004	0.00	0.054	0.16
Kyebxang Co	−0.0002	0.00	0.082 *	0.28

* Statistically significant at the 0.05 level; ** statistically significant at the 0.01 level.

4. Discussion

4.1. Water Volume (Depth and Area)

As demonstrated in Figures 3, 5 and 8, the area, depth and volume of water bodies have strong impacts on the variability of water temperature. According to [13], a strong relationship between heat budgets and water volume is possible for a specific lake. Thus, small temporal variations were revealed for lakes with large volume, e.g., Lake Qinghai, Nam Co and Siling Co, and Ayakekumu (Table 1). Similar reasons can be attributed to the lower value of DTDs for large volume lakes. This can also explain why Lake Langa Co showed larger temporal variability and DTD than that for Lake MapamYumco though these two lakes have very similar environmental settings (closely situated, almost same elevation, Table 2 and Figure S4). Lake Gyaring showed slightly higher variability and DTDs than Lake Ngoring, but the difference is insignificant. Thereby, other factors (e.g., the ratio of area to mean depth, and shoreline characteristic) may contribute to this phenomenon, and further investigation is required to determine the underlying reasons [29,30]. As the extreme case, Lake Dabsun exhibited the highest temperature (Max: 25.1 °C; Mean of ice-free season, MIFS: 15.54°C), which is also the shallowest (around 1 m) lake at lowest elevation (2678 m). Given the elevation difference between Lake Qinghai and Dabsun (517 m), the air temperature is about 3 °C, which is much smaller than the corresponding averaged LWST difference during the ice-free season (15.54 − 9.09 = 6.45 °C). Thereby, the highest temperature observed for Lake Dabsun is also attributed to its shallow water depth with small water storage.

4.2. Elevation and Air Temperature

As shown in Figures 3–5, the LWST of Lake Qinghai (15.8) is higher than that of Lake Nam Co (11.3) for both daytime and nighttime results. Similarly, Lake Yamdrok (Elevation: 4441 m; Area: 630 km^2; Depth: 20–40 m) and Lake PumuYumco (Elevation: 5003 m; Area: 295 km^2, 30–40 m) both are located in the southern part of the plateau, but the former has much higher temperature. According to [8] and [13], larger volume lakes exhibit higher heat budget, meaning that Lake Qinghai should show lower temperature than Lake Nam Co, the same conclusion holds for Lakes Yamdrok and PumuYumco. However, an opposite trend was observed mainly due to high elevation resulting in low air temperature, which leads to cool lake water. The air temperature lapse rate for the mountainous area with elevation ranging from 2000 to 6000 m is about 5–6 °C/1000 m [31], thus the difference of elevation for these two pairs of lakes may be one of the predominant reasons for the difference of temperature. To further investigate the relationship between air temperature over lakes and LWST, a regression model for air

temperature over lake against MODIS derived lake surface temperature was obtained for each lake (see Figure S6 for the details of the data source and data extraction methods). As shown in Figure 10, close correlation was obtained for daytime, nighttime and the mean temperature. Examination of the correlation for each lake revealed strong effects of air temperature on LWST for lakes surrounded by homogeneous landscape (Lake Dabsun, and Lake Qinghai), while relatively weak relationships were obtained for lakes surrounded with heterogeneous landscape (MapamYumco, and Langa Co). One extreme case was Lake Xuru Co, which might be influenced by other factors, e.g., water salinity and hot spring ground water supplies. Further investigation was needed to determine the reasons. As shown in Figure 11, the monthly air temperature of lakes distributed over the plateau co-varies very well with their LWST (see Figure S4 for locations) in most of the cases. However, the air temperatures were much lower than the LWST derived from the MODIS LST product, which is probably due to narrow lake shorelines and complex reliefs around these lakes (Figure 11c,e,f). Thus, the footprint of the interpolated air temperature may contain land surface exhibiting gradient air temperature variations, particularly those lakes surrounded by elevated mountains, which showed a large discrepancy between air temperature and LWST derived from MODIS LST product.

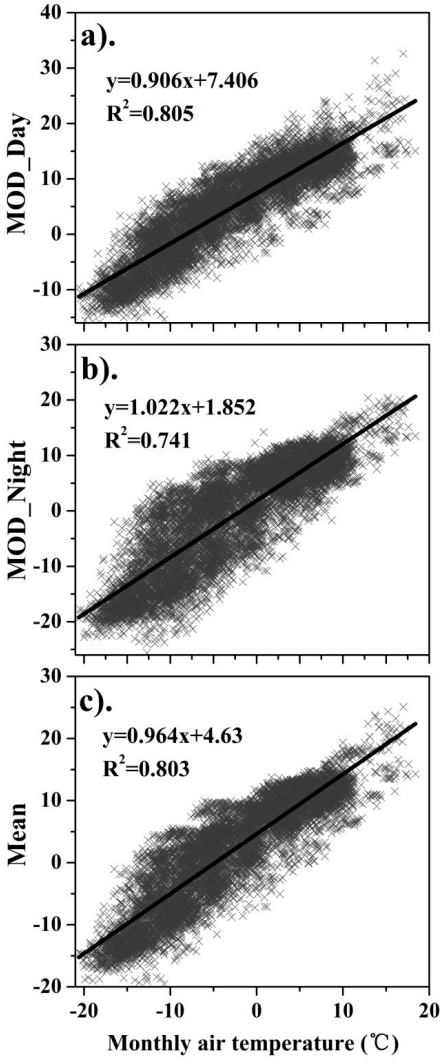

Figure 10. The relationships between monthly air temperature over lakes and averaged monthly lake surface temperature (WST) derived from MODIS images from 2001 to 2015: (**a**) daytime; (**b**) nighttime; and (**c**) mean WST of daytime and nighttime values.

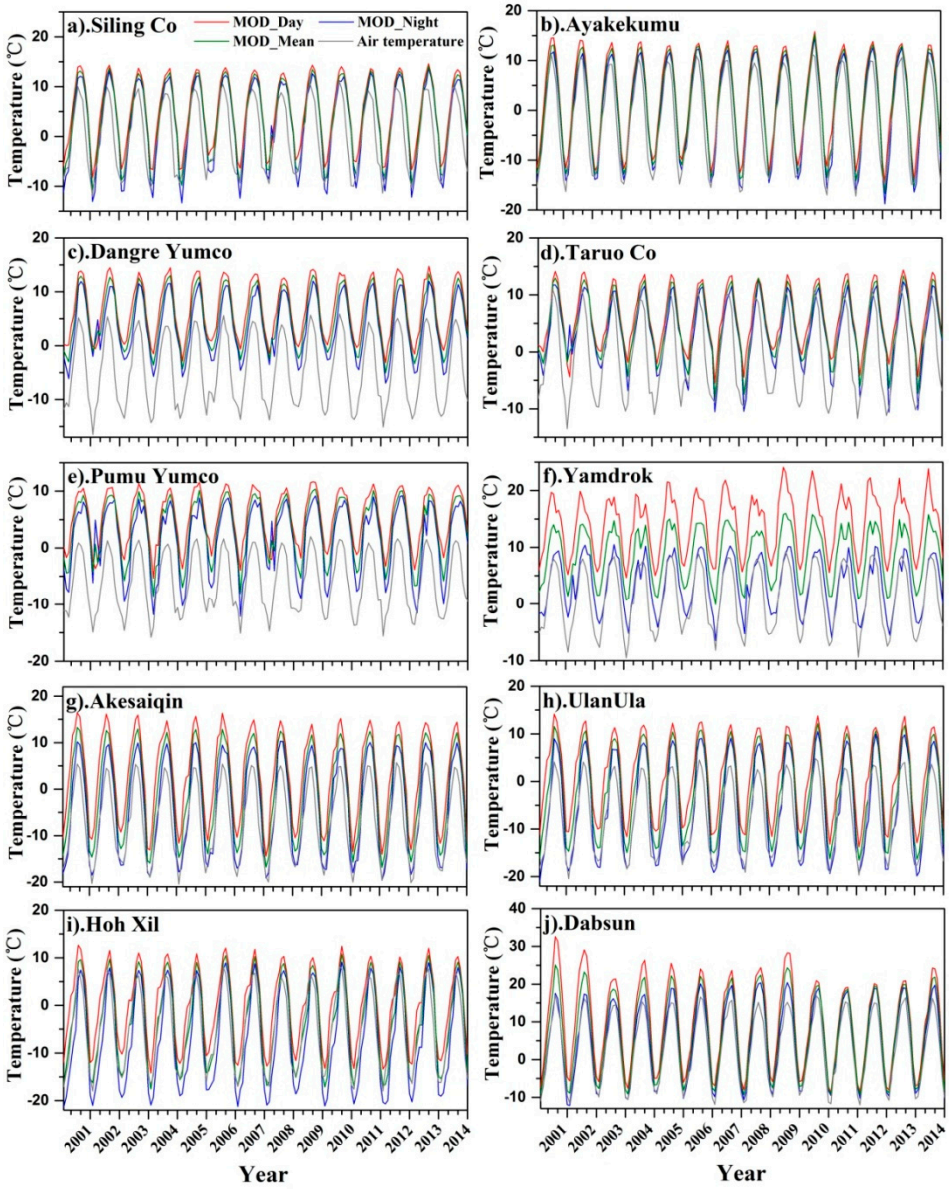

Figure 11. The variations of monthly air temperature over lakes and averaged monthly lake surface temperature derived from MODIS images during 2000 to 2015: (**a**) Siling Co; (**b**) Aykekumu; (**c**) DangreYumco; (**d**) Taruo Co; (**e**) PumuYumco; (**f**) Yamdrok; (**g**) Akesaiqin; (**h**) UlanUla; (**i**) Hoh Xil; and (**j**) Dabsun.

4.3. Water Supply Sources and Salinity

Lake Ayakekumu is located in relatively low elevation (3876 m), but its LWST is low compared with lakes in the similar elevation with the same depth (10 m). Feeding with snow and glacier melting water, the lake has shown an obvious areal increase in the past 26 years (Figure S7). A low temperature is expected as the mainly water supply to the lake originates from melting glaciers. Likewise, mainly supplied by glacier and snow melting waters [32,33], low temperatures were recorded in Lake HolXil (Max: 8.47 °C; Mean of ice-free season, MIFS: 6.20 °C) and Lake LexieWudan (Max: 8.52·°C; MIFS: 5.51 °C) (see Figure S4 for locations). Situated in almost the same elevation, Lake UlanUla (Max: 10.25 °C; MIFS: 7.32 °C) and XijinUlan (Max: 10.69 °C; MIFS: 7.71 °C) had higher temperature. In addition, Lake HolXil and LexieWudan had a much shorter ice-free period being 136 and 160 days, respectively; comparatively, Lake UlanUla and XijinUlan showed a longer ice-free period (192 days and 168 days,

respectively). These four lakes have very similar elevation and climatic conditions, the water supply source may be the major reason for their difference in temperature. Further, most the lakes with decreased temperature change rate are also more or less related to water supplying source, which is consistent with the findings by [20]. As known that the water salinity has effects on ice formation temperature, thus elongated ice-free duration may be expected for these high salinity lakes [34]. These hypothesis need to be further investigated on the saline effect on water temperature and ice-free duration.

5. Conclusions

The inter-annual and intra-annual variations of WST for lakes across the Tibetan Plateau were derived from 1472 (7360 tiles) maps of daytime and nighttime MODIS LST eight-day composites during the period 2000–2015. The descriptive statistics of ice break-up, warm month, and ice freeze-up LWST and annual cycles of overall lakes and typical lakes were determined from the MOSDIS LST eight-day composite for 56 lakes greater than 50 km^2 over the plateau. The annual cycle of LWST ranged from −19.5 °C in February to 25.1 °C in July. In terms of the spatial variation for typical seasons, the LWST ranged from −4 to 8.7 °C in the ice break-up season, from 8.3 to 25.1 °C in warm months (the end of July to beginning of August), and 13.7 to −2.4 °C in the freeze-up season. Much smaller DTDs were exhibited in summer and autumn, ranging from 1.3 to 8.9 °C, while larger DTDs were revealed in ice break-up season, ranging from 2.5 to 16.6 °C. This investigation also revealed that no obvious temperature change pattern can be determined for the 56 lakes being examined during the past 15 years. However, the inter-annual temperature variations measured from daytime and nighttime MODIS LST data showed different trends, and only 23 (41%) lakes showed either increasing or decreasing temperature trend from both daytime and nighttime measurements. According to the daytime MODIS LST measurements, 20 lakes exhibited a change rate of LWST, which was statistically significant, including three warming and 16 cooling lakes; 21 lakes showed a statistically significant rate of temperature change, but included eight warming and 13 cooling lakes for the nighttime MODIS LST measurements. It should also be highlighted that the spanning time may exert impacts on the inter-annual LWST change rate. According to this investigation, several factors, e.g., lake depth and area (volume), attitude, and water supply source can contribute to the spatiotemporal variation of LWST for lakes across the Tibetan Plateau. Shallow lakes contribute to a rapid response of SWT to solar and atmospheric forcing, while the response of large deep lakes is much slow. In addition, water salinity and ground water supply might be potential factors influencing LWST and ice-free duration, which need further investigation.

Supplementary Materials: The following are available online at www.mdpi.com/2072-4292/8/10/854/s1, Figure S1: Before and after-filtering of MODIS LST 46 8-day composites from two typical pixels extracted from lake area; Figure S2: The percentage of valid pixels for day and night time MODIS LST images from 2000 to 2015 (1472 mosaics); Figure S3: Statistics of effective images for MODIS LST products across the Tibetan Plateau during 2000–2015, where the white gap indicates no MODIS LST data meets the valid pixels greater than 76; Figure S4: The names and locations of typical lakes concerned across the Tibetan Plateau in this investigation; Figure S5: (a) Inter-annual changes of lake-averaged annual daytime, nighttime and mean water surface temperature (WST) of Lake Siling Co from 2000 to 2015; and (b) nighttime trend from 2001 to 2013; Figure S6: Monthly air temperature product derived from data provided by China Meteorological Administration at a grid resolution of 0.5 degree, lake boundary shape file overlaid to the interpolated monthly air temperature product (the left column), and comparison of the extracted air temperature with lake surface temperature derived from MODIS LST product with example from Lake Ayakekumu (right column), (a)–(c) are air temperature versus daytime, nighttime and the average of daytime and nighttime MODIS LST over lake surface; Figure S7: Water surface area variation for Lake Ayakekumu from 1989 to 2015 retrieved with Landsat TM imagery data acquired in August or September for each year with data available. Table S1: There are 34 lakes match from both studies, and 10 lakes show lake surface temperature increase and 8 show lake surface temperature decrease from both studies; while the rest 16 lakes demonstrate different trend, however, if we narrow the LWST from 2001 to 2012, 8 more lakes show consistent LWST trend, and the remaining 8 lakes show different tend, however, these lakes generally did not show obvious trend according to the determination coefficient (R^2) values.

Acknowledgments: The authors would like to thank financial supports from Natural Science Foundation of China (No. 41471290), and "One Hundred Talents" Program from Chinese Academy of Sciences granted to Kaishan Song. Thanks are extended to NASA for providing free MODIS LST imagery data. Many thanks also go to the editor and three anonymous reviewers for their valuable and instructive comments that have strengthened the manuscript. At last, the authors would like to thank Lin Li from Indiana Purdue University, Indianapolis (IUPUI) for improving the English expression, and Jingjing Zang, Yanqiu Li, and Junbin Hou for their valuable assistances in data collection and preprocessing.

Author Contributions: K.S. and Y.Y. conceived and designed the analysis; Y.Y., M.W., J.D., J.M., M.W., and G.M. analyzed the data; K.S. wrote the paper; K.S. and M.W. revised the paper.

Conflicts of Interest: The authors declare no conflict of interest.

References

1. Li, R.N.; Chen, Q.W.; Zhang, X.Q.; Recknagel, R. Effects of temperature and macronutrients on phytoplankton communities across three largely different lakes identified by a time-space trade-off approach. *Ecol. Inform.* **2015**, *29*, 174–181. [CrossRef]
2. Ma, N.; Szilagyi, J.; Niu, G.Y.; Zhang, Y.S.; Zhang, T.; Wang, B.B.; Wu, Y.H. Evaporation variability of Nam Co Lake in the Tibetan Plateau and its role in recent rapid lake expansion. *J. Hydrol.* **2016**, *537*, 27–35. [CrossRef]
3. Verburg, P.; Hecky, R.E.; Kling, H. Ecological consequences of a century of warming in Lake Tanganyika. *Science* **2003**, *301*, 505–507. [CrossRef] [PubMed]
4. Schneider, P.; Hook, S.J. Space observations of inland water bodies show rapid surface warming since 1985. *Geophys. Res. Lett.* **2010**. [CrossRef]
5. Adrian, R.; O'Reilly, C.M.; Zagarese, H.; Baines, S.B.; Hessen, D.O.; Keller, W.; David, M.L.; Ruben, S.; Dietmar, S.; Ellen, V.D.; et al. Lakes as sentinels of climate change. *Limnol. Oceanogr.* **2009**, *54*, 2283–2297. [CrossRef] [PubMed]
6. Livingstone, D.M. Impact of secular climate change on the thermal structure of a large temperate central European lake. *Clim. Chang.* **2003**, *57*, 205–225. [CrossRef]
7. Hampton, S.; Izmesteva, L.R.; Moore, M.V.; Katz, S.L.; Dennis, B.; Silow, E.A. Sixty years of environmental change in the world's largest freshwater lake—Lake Baikal, Siberia. *Glob. Chang. Biol.* **2008**, *14*, 1947–1958. [CrossRef]
8. Wetzel, R.G. *Limnology: Lake and River Ecosystems*, 3rd ed.; Elsevier Academic Press: New York, NY, USA, 2001.
9. Hulley, G.C.; Hook, S.J.; Schneider, P. Optimized split-window coefficients for deriving surface temperatures from inland water bodies. *Remote Sens. Environ.* **2011**, *115*, 3758–3769. [CrossRef]
10. Alsdorf, D.E.; Lettenmaier, D.P. Tracking fresh water from space. *Science* **2003**, *301*, 1491–1494. [CrossRef] [PubMed]
11. Hook, S.; Vaughan, R.G.; Tonooka, H.; Schladow, S. Absolute radiometric in-flight validation of mid infrared and thermal infrared data from ASTER and MODIS on the terra spacecraft using the Lake Tahoe, CA/NV, USA, automated validation site. *IEEE Trans. Geosci. Remote Sens.* **2007**, *45*, 1798–1807. [CrossRef]
12. Ke, L.H.; Song, C.Q. Remotely sensed surface temperature variation of an inland saline lake over the central Qinghai—Tibet Plateau. *ISPRS J. Photogram. Remote Sens.* **2014**, *98*, 157–167. [CrossRef]
13. Gorham, E. Morphometric control of annual heat budgets in temperate lakes. *Limnol. Oceanogr.* **1964**, *9*, 529–533. [CrossRef]
14. Livingstone, D. Ice break-up on southern Lake Baikal and its relationship to local and regional air temperatures in Siberia and the North Atlantic Oscillation. *Limnol. Oceanogr.* **1999**, *44*, 1486–1497. [CrossRef]
15. Reinart, A.; Reinhold, M. Mapping surface temperature in large lakes with MODIS data. *Remote Sens. Environ.* **2008**, *112*, 603–611. [CrossRef]
16. Bussières, N.; Verseghy, D.; MacPherson, J.I. The evolution of AVHRR-derived water temperatures over boreal lakes. *Remote Sens. Environ.* **2002**, *80*, 373–384. [CrossRef]
17. Trumpickas, J.; Shuter, B.J.; Minns, C.K. Forecasting impacts of climate change on Great Lakes surface water temperatures. *J. Gt. Lakes Res.* **2009**, *35*, 454–463. [CrossRef]
18. Trumpickas, J.; Shuter, B.J.; Minns, C.K.; Cyr, H. Characterizing patterns of nearshore water temperature variation in the North American Great Lakes and assessing sensitivities to climate change. *J. Gt. Lakes Res.* **2015**, *41*, 53–64. [CrossRef]

19. Crosman, E.T.; Horel, J.D. MODIS-derived surface temperature of the Great Salt Lake. *Remote Sens. Environ.* **2009**, *113*, 73–81. [CrossRef]
20. Zhang, G.; Yao, T.; Xie, H.; Qin, J.; Ye, Q.; Dai, Y.; Guo, R. Estimating surface temperature changes of lakes in the Tibetan Plateau using MODIS LST data. *J. Geophys. Res. Atmos.* **2014**, *119*, 8552–8567. [CrossRef]
21. Zhou, B.; Xu, Y.; Wu, J.; Dong, S.; Shi, Y. Changes in temperature and precipitation extreme indices over China: Analysis of a high-resolution grid dataset. *Int. J. Climatol.* **2015**. [CrossRef]
22. Song, C.Q.; Huang, B.; Ke, L.H.; Richards, K.S. Seasonal and abrupt changes in the water level of closed lakes on the Tibetan Plateau and implications for climate impacts. *J. Hydrol.* **2014**, *514*, 131–144. [CrossRef]
23. Rangwala, I.; Miller, J.R.; Xu, M. Warming in the Tibetan Plateau: Possible influences of the changes in surface water vapor. *Geophys. Res. Lett.* **2009**. [CrossRef]
24. Zhang, G.; Xie, H.; Kang, S.; Yi, D.; Ackley, S.F. Monitoring lake level changes on the Tibetan Plateau using ICESat altimetry data (2003–2009). *Remote Sens. Environ.* **2011**, *115*, 1733–1742. [CrossRef]
25. Xiao, F.; Ling, F.; Du, Y.; Feng, Q.; Yan, Y.; Chen, H. Evaluation of spatial temporal dynamics in surface water temperature of Qinghai Lake. *J. Arid Land* **2013**, *5*, 452–464. [CrossRef]
26. Wan, Z.; Zhang, Y.; Zhang, Q.; Li, Z.L. Validation of the land surface temperature products retrieved from terra moderate resolution imaging spectroradiometer data. *Remote Sens. Environ.* **2002**, *83*, 163–180. [CrossRef]
27. Schneider, P.; Hook, S.J.; Radocinski, R.G.; Corlett, G.K.; Hulley, G.C.; Schladow, S.G.; Steissberg, T.E. Satellite observations indicate rapid warming trend for lakes in California and Nevada. *Geophys. Res. Lett.* **2009**. [CrossRef]
28. Coll, C.; Caselles, V.; Galve, J.M.; Valor, E.; Niclos, R.; Sanchez, J.M.; Rivas, R. Ground measurements for the validation of land surface temperatures derived from AATSR and MODIS data. *Remote Sens. Environ.* **2005**, *97*, 288–300. [CrossRef]
29. Leblanc, M.; Lemoalle, J.; Bader, J.C.; Tweed, S.; Mofor, L. Thermal remote sensing of water under flooded vegetation: New observations of inundation patterns for the 'Small' Lake Chad. *J. Hydrol.* **2011**, *404*, 87–98. [CrossRef]
30. Austin, J.A.; Colman, S.M. Lake Superior summer water temperatures are increasing more rapidly than regional air temperatures: A positive ice-albedo feedback. *Geophys. Res. Lett.* **2007**. [CrossRef]
31. Jacobson, M.Z. *Fundamentals of Atmospheric Modeling*, 2nd ed.; Cambridge University Press: London, UK, 2005.
32. Lei, Y.B.; Yao, T.D.; Bird, B.W.; Yang, K.; Zhai, J.Q.; Sheng, Y.W. Coherent lake growth on the central Tibetan Plateau since the 1970s: Characterization and attribution. *J. Hydrol.* **2013**, *483*, 61–67. [CrossRef]
33. Magnuson, J.J.; Webster, K.E.; Assel, R.A.; Bowser, C.J.; Dillon, P.J.; Eaton, J.G.; Evans, H.E.; Fee, E.J.; Hall, R.I.; Mortsch, L.R.; et al. Potential effects of climate changes on aquatic systems: Laurentian Great Lakes and Precambrian Shield region. *Hydrol. Process.* **1997**, *11*, 825–871. [CrossRef]
34. Wang, S.M.; Dou, H.S. *Chinese Lakes Inventory*; Science Press: Beijing, China, 1998.